Modulation of Thrombin–Fibrinogen Interaction by Specific Ion Effects†

Raimondo De Cristofaro and Enrico Di Cera*

Department of Biochemistry and Molecular Biophysics, Washington University School of Medicine, Box 8231, St. Louis, Missouri 63110

Received July 9, 1991; Revised Manuscript Received August 28, 1991

ABSTRACT: Steady-state measurements of synthetic substrate hydrolysis by human α-thrombin in the presence of human fibrinogen, under experimental conditions where light scattering due to the formation of fibrin aggregates is negligible, have allowed for a quantitative evaluation of K_m for fibrinogen. Measurements of K_m for fibrinogen carried out at pH 7.5 and 37 °C as a function of NaCl, NaBr, KCl, and KBr concentration, from 50 to 500 mM, show that the derivative d ln K_m/d ln $a_\pm$, where $a_\pm$ is the mean ion activity, is constant over the entire range of salt concentrations and is strictly dependent on the particular salt present in solution. The values of d ln K_m/d ln $a_\pm$ are found to be equal to 0.75 ± 0.03 (NaCl), 0.90 ± 0.01 (NaBr), 0.62 ± 0.07 (KCl), and 0.60 ± 0.03 (KBr). Measurements of K_m for two synthetic amide substrates, under identical solution conditions, reveal practically no change in K_m with salt concentration, while they show a significant decrease in k_{cat} when Na^+ salts are replaced by K^+ salts. The drastic difference in the salt dependence of K_m between fibrinogen and the synthetic amide substrate points out that a significant role may be played by the fibrinogen recognition site in the energetics of thrombin–fibrinogen interaction. The sensitivity of K_m for fibrinogen to different salts unequivocally demonstrates that specific ion effects, rather than nonspecific ionic strength effects, modulate thrombin–fibrinogen interaction under experimental conditions of physiological relevance. Analysis of ion effects on clotting curves obtained at pH 7.5 and 37 °C also shows a drastic differential effect of cations and anions. The clotting time is minimum in the presence of NaCl and increases significantly in the presence of NaBr, KCl, or KBr.

The last enzymatic step of the coagulation cascade involves the interaction of thrombin with fibrinogen and triggers the formation of an insoluble gel of fibrin polymers. The extreme biological importance of such a reaction has long motivated investigation of its underlying physicochemical aspects (Sturtevant et al., 1955; Scheraga & Laskowski, 1957; Laki & Gladner, 1964; Doolittle, 1973, 1984; Hantgan & Hermans, 1979; Martinelli & Scheraga, 1980; Mihaly, 1968, 1988a,b; Dietler et al., 1986). Elegant studies of light scattering have characterized the physical steps involved in the early stages of fibrin polymerization (Hantgan & Hermans, 1979). Thorough high-performance liquid chromatography (HPLC)[1] analysis of the kinetics of release of fibrinopeptides subsequent to thrombin–fibrinogen interaction has revealed important aspects of this reaction (Martinelli & Scheraga, 1980; Mihaly, 1988b). More recently, the structural aspects responsible for the specificity of thrombin reaction with fibrinogen have begun to emerge (Bode et al., 1989; Rydel et al., 1990). A unique feature of thrombin is the fibrinogen recognition site (FRS) located in a structural domain close to the catalytic pocket and packed with a number of positive charges and hydrophobic residues. Gross structural perturbations and chemical modifications of the FRS dramatically lower or completely abolish thrombin clotting activity (Hofsteenge et al., 1988; Braun et al., 1989; Griffith, 1979; Church et al., 1989). Macromolecular effectors, such as hirudin, that bind to the FRS inhibit fibrinogen binding to thrombin in a competitive fashion (Stone & Hofsteenge, 1986), and so do other effectors specifically tailored to interact with the FRS (Di Maio, 1990; Maraganore et al., 1990). All these findings provide broad, albeit qualitative picture of the physicochemical aspects underlying thrombin–fibrinogen interaction. A quantitative understanding of the detailed components of this physiologically important reaction demands a thorough investigation of the thermodynamic driving forces underlying the structural changes of functional significance. Experimental studies of thrombin–fibrinogen interaction over a wide range of solution conditions are necessary to resolve these thermodynamic components. Understanding the thermodynamic driving forces responsible for the macromolecular interactions is also a prerequisite for the design and meaningful practical application of synthetic peptides capable of interfering with thrombin function in vivo.

In this paper, we introduce an experimental strategy whereby some basic aspects of thrombin–fibrinogen interaction can be explored over a wide range of solution conditions. The richness of charged residues that seem to be involved in fibrinogen recognition by thrombin (Bode et al., 1989; Rydel et al., 1990) makes the thermodynamic analysis and experimental investigation of ion effects particularly timely and important. Specific ion effects include preferential binding of cations and anions. They are expected to be different with different salts and are extremely sensitive to temperature changes (Tanford, 1962; Manning, 1969). Nonspecific, ionic strength effects arise as a result of possible influences of the salt on the activity coefficients of water, substrate, and the various forms of the macromolecular components and include Debye–Hückel screening effects. These effects only depend on the mean ion activity, $a_\pm$, or the ionic strength of the medium. They are independent of the particular salt present

† This work was supported in part by National Institutes of Health Research Grant RR 05389 and by a grant from the Lucille P. Markey Charitable Trust.

* Address correspondence to this author.

[1] Abbreviations: Chromozym-TH, tosyl-Gly-Pro-Arg-*p*-nitroanilide-AcOH; HPLC, high-performance liquid chromatography; PEG, poly(ethylene glycol); SDS–PAGE, sodium dodecyl sulfate–polyacrylamide gel electrophoresis; S-2238, H-D-Phe-pipecolyl-Arg-*p*-nitroanilide; Tris, tris(hydroxymethyl)aminomethane.

0006-2960/92/0431-257$03.00/0

in solution and change very little with temperature (Tanford, 1962; Manning, 1969; Record et al., 1978). Therefore, a meaningful discrimination between specific and nonspecific ion effects on thrombin–fibrinogen interaction necessarily demands experimental studies to be conducted in the presence of different salts, which is the purpose of this paper to report.

Materials and Methods

Thrombin and Fibrinogen Preparation. Human thrombin was provided by Dr. John W. Fenton, II (New York Department of Health, Albany, NY), as a mixture of α (81%), β (17%), and γ (2%) derivatives. Contaminant β- and γ-thrombins were eliminated by ion-exchange chromatography on Bio-Rex 70 as described elsewhere (Di Cera et al., 1991). The preparation of human α-thrombin was 99% pure as judged by SDS–PAGE on 5–25% gradient gels run under both reducing and nonreducing conditions. Thrombin concentration was measured using an extinction coefficient E_{280} = 1.83 mL mg^{-1} cm^{-1} and a molecular mass of 36.5 kDa (Fenton et al., 1977). The concentration determined spectrophotometrically matched the active-site concentration determined by titration with *p*-nitrophenylguanidinobenzoate hydrochloride (Chase & Shaw, 1967). Thrombin solutions of 2 μM concentration were stored in 50-μL vials at −80 °C until use. Human fibrinogen (grade L) was purchased form KabiVitrum (Stockholm, Sweden) and dissolved at 25 °C in distilled water to yield a solution with a final concentration in the range of 40–80 μM. Since the product from KabiVitrum typically contains NaCl, citrate, and other macromolecular components such as fibronectin, plasmin, and plasminogen, the solution of fibrinogen was first desalted using a Bio-Rad Econo-Pac 10DG column equilibrated with the buffer to be used in the functional studies, without any added salt. The protein content of the eluted fractions was detected by absorbance readings at 280 nm. The presence of contaminating salt in the pooled fractions was carefully checked as follows. The conductivity of reference solutions of NaCl (0.5–500 mM) in the same buffer was measured by means of an Orion Research 160 conductivitymeter at 25 °C. A linear plot of conductivity readings (in microsiemens per centimeter) as a function of salt concentration was obtained. The conductivity of each fraction eluted from the Bio-Rad column was then measured in an analogous way, and an excellent separation was found. The maximum amount of contaminating salt in the pooled fractions containing the protein never exceeded 1 mM, which is 2% of the lowest salt concentration used in the functional studies. Contaminant macromolecular components such as fibronectin, plasmin, and plasminogen were then eliminated by affinity chromatography on 5-mL columns of gelatin– and lysine–agarose (Deutsch & Mertz, 1970; Engvall et al., 1978), equilibrated with the buffer to be used experimentally. The purity of the fibrinogen preparation was tested by SDS–PAGE on 10–25% gradient gels run under both reducing and nonreducing conditions and found to be greater than 99%. Fibrinogen concentration was measured using an extinction coefficient E_{280} = 1.506 mL mg^{-1} cm^{-1} in 0.3 M NaCl and a molecular mass of 340 kDa (Mihaly, 1968). Fibrinogen solutions to be used in steady-state measurements were freshly made from powder each time according to the procedure described above, while those to be used in clotting assays were stored at −80 °C in 70-μL vials, at a concentration of 2 μM, until use.

Steady-State Measurements. Steady-state measurements of human α-thrombin amidase activity were made using the synthetic chromogenic peptide S-2238 purchased from KabiVitrum (Stockholm, Sweden). The concentration of S-2238 was carefully measured at 342 nm using a Cary 3 dual-beam spectrophotometer before and after each experimental determination. All assays were performed by following the release of *p*-nitroaniline resulting from the hydrolysis of S-2238 as an increase in absorbance at 405 nm using a Cary 3 dual-beam spectrophotometer. The concentration of released *p*-nitroaniline was quantified by means of appropriate extinction coefficients as reported elsewhere (Di Cera et al., 1991). Assays were performed using disposable polystyrene cuvettes under solution conditions of 50 mM Tris and 0.1% PEG 8000, pH 7.5 and 37 °C, in the presence of the desired concentration of salt. Addition of PEG 8000 was to prevent absorption of the enzyme to the cuvette walls. Thrombin concentration was 1 nM in all assays. The buffer solution was titrated at pH 7.5 using an Orion Research EA 940 expandable ion analyzer equipped with an automatic temperature compensation probe. Additions of HCl were used in studies involving NaCl and KCl, while HBr was used in those involving NaBr and KBr.

Steady-state measurements of substrate hydrolysis were carried out in the presence of fibrinogen used as a competitive inhibitor to obtain K_m and k_{cat} for the synthetic substrate, along with K_m for fibrinogen. These parameters were resolved from analysis of experimental data (see Data Analysis) obtained according to the following strategy. Eight curves of substrate hydrolysis were measured, using seven substrate concentrations scaled by a factor of 2 in a range typically from 0.5 to about 50 μM. One curve was measured in the absence of fibrinogen, and seven other curves were collected in the presence of fibrinogen concentrations scaled by a factor of 1.5. The highest fibrinogen concentration was typically within $^1/_2$–$^1/_3$ of the K_m value measured experimentally. Velocity measurements of substrate hydrolysis taken over an interval of 60 s (3 points/s) were used to calculate initial rates by linear least squares of the linear portion of the product formation curve. The linear portion typically spans 15–60 s, depending upon substrate concentration. The KINETICS software of the Cary 3 spectrophotometer was used for linear least squares. Analysis of the linear portion of the progress curve guarantees a meaningful measurement of initial rates and is aimed at avoiding any complicating effects, arising from significant substrate depletion and inhibition by product, that induce departure from linear behavior. The accuracy of initial rate measurements was demonstrated by the very high values of the correlation coefficient ($r > 0.99$ in all cases) obtained for the fit over the linear portion of the progress curves run as a function of substrate concentration.

A complication to be overcome in these studies is that scattering due to fibrin polymerization subsequent to fibrinogen hydrolysis by thrombin can interfere with the increase in absorbance at 405 nm due to the hydrolysis of synthetic substrate. This point, which seems to have been overlooked in previous studies (Lundblad et al., 1984; Lord et al., 1990), was given much consideration in the present study. For each fibrinogen concentration used, a clotting curve was measured at 405 nm in the absence of synthetic substrate to assess the contribution arising from scattering over the time scale of 60 s used in steady-state determinations. The increase in turbidity at 405 nm due to scattering was typically found to be linear and interpolated as an apparent rate of hydrolysis using the KINETICS software of the Cary 3 spectrophotometer. The apparent rate computed in this way gave the maximum possible contribution arising from scattering, since the presence of synthetic substrate can only decrease the amount of fibrinogen converted to fibrin per unit time. The information collected from the clotting curves was used to weight data points dif-

ferentially in nonlinear least squares (see Data Analysis).

Salt effects on the thrombin–fibrinogen interaction were studied under conditions of 50 mM Tris, pH 7.5 at 37 °C, using NaCl, KCl, NaBr, or KBr over a concentration range from 50 to 500 mM. These salts were chosen to yield a self-contained set of measurements where each cation is used with two different anions and vice versa. The mean ion activity $a_\pm = \sqrt{\gamma_+\gamma_-c_+c_-}$, where c_+ and c_- are the concentrations of the cation and anion, respectively, was computed from the values of activity coefficients reported elsewhere (Lewis & Randall, 1961) and interpolated according to the equation:

$$\gamma = \alpha_1 c + \alpha_2 c^2 + \alpha_3 c^3 \quad (1)$$

where γ is the activity coefficient, c the ion concentration, $\alpha_1 = 0.772 \pm 0.013$, $\alpha_2 = -0.083 \pm 0.039$, and $\alpha_3 = 0.122 \pm 0.027$. The equation above is accurate within 0.0026 unit and was used for the calculation of either γ_+ or γ_- from c_+ and c_-. This is consistent with the widely accepted assumption that the dependence of the activity coefficient, γ, on the ion concentration, c, is the same for all ions (Record et al., 1978; Lohman, 1985).

Data Analysis. Competition experiments of synthetic substrate hydrolysis in the presence of fibrinogen can be analyzed in terms of a kinetic scheme where the free enzyme, E, interacts with either the synthetic substrate, S, or fibrinogen, F:

$$E + S \underset{{}^{S}k_{-1}}{\overset{{}^{S}k_1^*}{\rightleftharpoons}} ES \xrightarrow{{}^{S}k_2} E + P \quad (2a)$$

$$E + F \underset{{}^{F}k_{-1}}{\overset{{}^{F}k_1^*}{\rightleftharpoons}} EF \xrightarrow{{}^{F}k_2} E + P' \quad (2b)$$

where P and P′ are the products of the two reactions, k_2 is the rate-limiting acylation, and k_1^* and k_{-1} are the rate constants for substrate binding and dissociation, respectively (Di Cera et al., 1991). The superscripts S and F refer to the synthetic substrate and fibrinogen, respectively. The steady-state velocity of product formation in the first reaction, $v = d[P]/dt$, is given by (Rubinow & Lebowitz, 1970; Segel, 1988)

$$v = e_T \frac{{}^{S}k_{cat}[S]}{{}^{S}K_m(1 + [F]/{}^{F}K_m) + [S]} \quad (3)$$

where e_T is thrombin concentration, ${}^{S}k_{cat} = {}^{S}k_2$, ${}^{S}K_m = ({}^{S}k_{-1} + {}^{S}k_2)/{}^{S}k_1^*$, and ${}^{F}K_m = ({}^{F}k_{-1} + {}^{F}k_2)/{}^{F}k_1^*$. Analysis of measurements of v as a function of [S], over a range of fibrinogen concentrations, yields the three independent parameters, ${}^{S}k_{cat}$ and ${}^{S}K_m$ for the synthetic substrate and ${}^{F}K_m$ for fibrinogen. Under each experimental condition analyzed in this study, eight curves of substrate hydrolysis were measured in a 7 × 8 matrix, using seven substrate concentrations scaled by a factor of 2 and eight fibrinogen concentration scaled by a factor of 1.5, with one curve measured in the absence of fibrinogen. All curves were globally analyzed according to eq 3 to resolve the 3 independent parameters from a total of 56 experimental data points. For each curve at a given fibrinogen concentration, the apparent velocity due to an increase in turbidity at 405 nm measured at the same fibrinogen concentration in the absence of substrate (see Steady-State Measurements) was compared to the steady-state velocity of substrate hydrolysis. All velocity measurements that did not exceed the apparent velocity due to scattering by at least a factor of 10 were weighted 0 in the minimization procedure. All other points were weighted uniformly. Minimization was accomplished by nonlinear least squares using the Marquardt method, and best-fit estimates were obtained by extensive search in the parameter space using different starting guesses. Convergence to a unique minimum was always obtained. Confidence intervals on the parameters were computed by F-testing at the cutoff of one standard deviation (68%). Point perturbation analysis of residuals (Di Cera et al., 1989) revealed no significant departure from random behavior in all cases.

Control Experiments. The consistency and robustness of the experimental strategy used in the determination of the parameters involved in the eq 2a,b were checked in a number of ways by control experiments and Monte Carlo simulations (see Results). The use of different preparations of human α-thrombin and fibrinogen yielded extremely reproducible results under all experimental conditions examined in this study. An important prediction drawn from the eq 2a and 2b is that the value of ${}^{F}K_m$ for fibrinogen determined in the competition experiments must be independent of the particular synthetic substrate used. Determinations of ${}^{F}K_m$ using S-2238 were found to overlap extremely well with those derived from experiments where Chromozym-TH, a different amide substrate, was used.

Measurements of the Clotting Curve. Clotting curves were measured as an increase in turbidity at 350 nm as a function of time using a Cary 3 dual-beam spectrophotometer. All assays were carried out under experimental conditions of 0.25 μM human fibrinogen, 50 mM Tris, and 0.1% PEG 8000, pH 7.5 at 37 °C, as a function of thrombin concentration and in the presence of 0.1 M NaCl, NaBr, KCl, or KBr. The clotting time, t_c, was determined from extrapolation of the maximum slope of the clotting curve to the absorbance base line, as described in detail elsewhere (De Cristofaro & Di Cera, 1991). This definition of the clotting time parallels the one derived from light-scattering experiments (Hantgan & Hermans, 1979), it has been shown to directly reflect the enzymatic events involved in clot formation and is proportional to the ratio K_m/V_{max} ($V_{max} = e_T k_{cat}$) for fibrinogen (De Cristofaro & Di Cera, 1991).

Results

A typical set of steady-state determinations of synthetic substrate hydrolysis in the presence of fibrinogen is shown in Figure 1. The best-fit parameters obtained by global analysis of the data along the lines discussed under Materials and Methods are listed in Table I. The results obtained by fitting each curve separately are also given in Table I. Analysis of these results according to the equation ${}^{S}K_m([F]) = {}^{S}K_m\{1 + [F]/{}^{F}K_m\}$ for competitive inhibition (Segel, 1988) gives values of ${}^{S}K_m = 7.6 \pm 0.2$ μM and ${}^{F}K_m = 14.4 \pm 1.9$ μM, in very good agreement with the values of ${}^{S}K_m = 7.5 \pm 0.1$ μM and ${}^{F}K_m = 13.3 \pm 1.1$ μM obtained from global analysis. The resolution of all parameters is very good, which shows the reliability of the strategy used to collect and analyze the steady-state data in the competition experiments. Experimental data have been collected according to this strategy in the presence of different salts, under standard conditions of 50 mM Tris and 0.1% PEG 8000, pH 7.5 at 37 °C. The reason for using these conditions is 2-fold: the pH and temperature are of potential physiological interest, and at 37 °C the complicating effects of scattering due to fibrin polymerization subsequent to fibrinogen cleavage by thrombin are negligible over the time scale (60 s) of steady-state measurements (De Cristofaro & Di Cera, 1991).

The effects of four different salts, NaCl, NaBr, KCl, and KBr, have been explored in the concentration range from 50 to 500 mM, and the kinetic parameters ${}^{S}k_{cat}$, ${}^{S}K_m$, and ${}^{F}K_m$ obtained from analysis of the experimental data according to

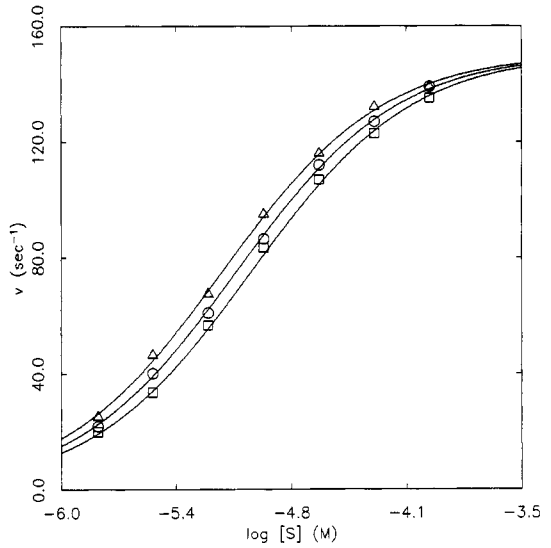

FIGURE 1: Typical steady-state measurements of synthetic substrate (S-2238) hydrolysis in the presence of human fibrinogen. The data are shown as velocity, normalized by thrombin concentration, as a function of the logarithm of substrate concentration. Data points were collected in a 7 × 8 matrix of substrate and fibrinogen concentrations. Only three out of eight curves are shown in the plot for the sake of clarity. Experimental conditions are 1 nM human α-thrombin, 50 mM Tris, 0.1% PEG 8000, and 0.25 NaCl, pH 7.5 and 37 °C. The concentration of human fibrinogen is (△) 0, (○) 2.2, and (□) 7.5 μM. Continuous lines were drawn from eq 3 using the best-fit parameter values obtained from global analysis, as listed in Table I.

Table I: Best-Fit Values of $^{S}K_m$, $^{S}k_{cat}$, and $^{F}K_m$ As Obtained from Global Analysis of Competition Experiments under Conditions of 1 nM Human α-Thrombin, 0.25 M NaCl, 50 mM Tris, and 0.1% PEG 8000, pH 7.5 at 37 °C[a]

Global Analysis				
[F] (μM)	$^{S}K_m$ (μM)	$^{S}k_{cat}$ (s^{-1})	$^{F}K_m$ (μM)	σ (s^{-1})
0–7.5	7.5 ± 0.1	150.4 ± 0.6	13.3 ± 1.1	1.6
Individual Analysis				
[F] (μM)	$^{S}K_m$([F]) (μM)	$^{S}k_{cat}$ (s^{-1})		σ (s^{-1})
0	7.4 ± 0.4	151.4 ± 2.2		2.4
0.7	7.8 ± 0.3	150.7 ± 1.4		1.5
1.0	7.9 ± 0.2	150.6 ± 1.3		1.4
1.5	8.1 ± 0.2	149.5 ± 1.2		1.2
2.2	9.0 ± 0.3	151.1 ± 1.5		1.5
3.3	9.4 ± 0.4	151.8 ± 1.8		1.8
5.0	9.6 ± 0.2	149.0 ± 0.8		0.8
7.5	10.5 ± 0.3	148.3 ± 1.3		1.2

[a] The best-fit values of $^{S}K_m([F]) = {}^{S}K_m\{1 + [F]/{}^{F}K_m\}$ obtained in the separate analysis of each curve of substrate hydrolysis, at a given fibrinogen concentration [F], are also given for comparison. Errors were computed by *F*-testing at the cutoff of one standard deviation (68%). σ is the standard error of the fit.

eq 3 are shown in Figures 2–4. The best-fit values of the parameters obtained under all solution conditions reported in this study are listed in Table II. The first important aspect that seems to emerge from these data is the striking difference in the salt dependence of the K_m for fibrinogen (Figure 2) with respect to the K_m for the synthetic substrates S-2238 and Chromozym-TH (Figure 3). Such a difference is not surprising and must reflect the contribution of differential structural components to thrombin interaction with its natural substrate fibrinogen and the synthetic amide substrates S-2238 and Chromozym-TH. Synthetic substrates are small compared to fibrinogen and bind only to the catalytic pocket of the enzyme, while fibrinogen binding involves also the FRS and probably triggers extensive structural modifications. Another important aspect arises in connection with the specificity of

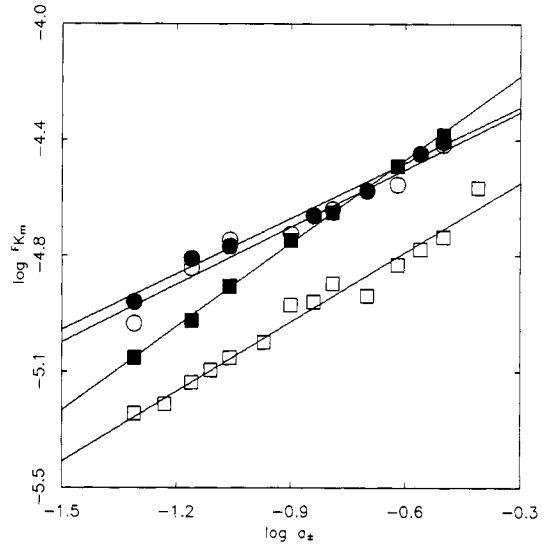

FIGURE 2: Experimental determinations of $^{F}K_m$ from the competition experiments reported in this study. The data are plotted as a function of the logarithm of mean ion activity, $a_{\pm}$, in the presence of (□) NaCl, (■) NaBr, (○) KCl, or (●) KBr. The values of $a_{\pm}$ were computed according to eq 1 in the text. Experimental conditions are 1 nM human α-thrombin, 50 mM Tris, and 0.1% PEG 8000, pH 7.5 and 37 °C. The slope of each straight line interpolating the experimental points for any given salt is 0.75 ± 0.03 (NaCl), 0.90 ± 0.01 (NaBr), 0.62 ± 0.07 (KCl), and 0.60 ± 0.03 (KBr). The values of $^{F}K_m$ under all salt conditions are listed in Table II.

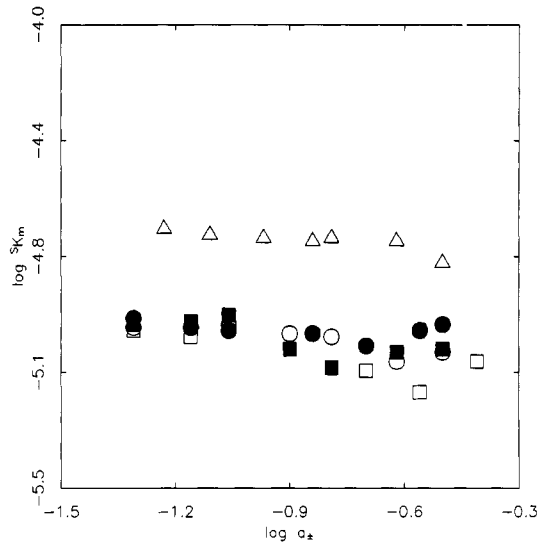

FIGURE 3: Experimental determinations of $^{S}K_m$ for the synthetic substrates S-2238 (□, ■, ○, ●) and Chromozym-TH (△) from the competition experiments reported in this study. The data are plotted as a function of the logarithm of mean ion activity, $a_{\pm}$, in the presence of (□, △) NaCl, (■) NaBr, (○) KCl, or (●) KBr. The values of $a_{\pm}$ were computed according to eq 1 in the text. Experimental conditions are 1 nM human α-thrombin, 50 mM Tris, and 0.1% PEG 8000, pH 7.5 and 37 °C. The values of $^{S}K_m$ under all salt conditions are listed in Table II.

the effects observed. It is clear that ion effects play a major role in controlling thrombin–fibrinogen interaction, as demonstrated by the significant dependence of $^{F}K_m$ on salt concentration. This is consistent with the structural observation that the FRS is coated by a patch of positively charged residues. It is also clear that such ion effects are specific, since they strongly depend on the particular salt present in solution. At any given value of the mean ion activity, $a_{\pm}$, the value of $^{F}K_m$ is minimum in the presence of NaCl. The logarithm of $^{F}K_m$ changes linearly with the logarithm of $a_{\pm}$, with a slope

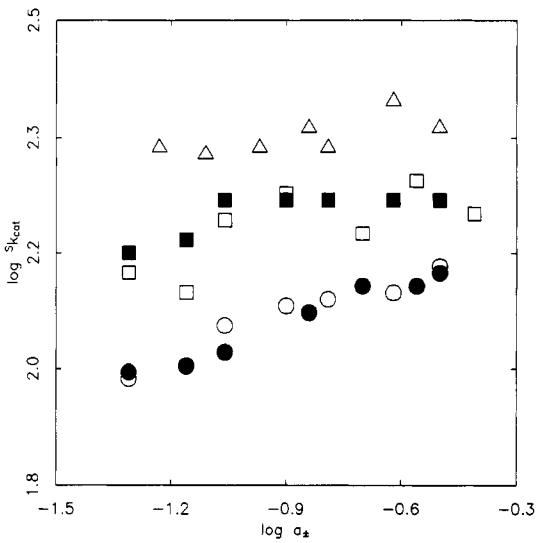

FIGURE 4: Experimental determinations of $^{S}k_{cat}$ for the synthetic substrates S-2238 (□, ■, ○, ●) and Chromozym-TH (△) from the competition experiments reported in this study. The data are plotted as a function of the logarithm of the mean ion activity, $a_{\pm}$, in the presence of (□, △) NaCl, (■) NaBr, (○) KCl, or (●) KBr. The values of $a_{\pm}$ were computed according to eq 1 in the text. Experimental conditions are 1 nM human α-thrombin, 50 mM Tris, and 0.1% PEG 8000, pH 7.5 and 37 °C. The values of $^{S}k_{cat}$ under all salt conditions are listed in Table II.

of 0.75 ± 0.03. The use of NaBr instead of NaCl leads to substitution of the anionic component in the presence of Na^+. This substitution not only nearly doubles the values of $^{F}K_m$ but also yields a slope of 0.90 ± 0.01, which is significantly higher than that observed with NaCl. The use of KCl again doubles the values of $^{F}K_m$ with respect to those observed with NaCl, but yields a slope of 0.62 ± 0.07, which is significantly smaller than that observed with NaCl. Interestingly, the substitution of the anionic component in the presence of K^+ does not lead to any significant change in either the values of $^{F}K_m$ or the slope. Thrombin–fibrinogen interaction is therefore very sensitive to different anions and cations. The system discriminates between Cl^- and Br^- in the presence of Na^+, but not in the presence of K^+. Analysis of the results reported in Figure 2 in terms of cationic substitutions points out that the system also discriminates between Na^+ and K^+, especially when Cl^- is present. These findings are incompatible with a description of the facts in terms of nonspecific, ionic strength effects and demand an interpretation in terms of specific binding interactions of cations and anions. Furthermore, since the discrimination between cations depends upon the particular anion present and vice versa, it is clear that specific interactions must exist among cation and anion binding sites.

The effects seen in the case of $^{S}K_m$ and $^{S}k_{cat}$ also deserve consideration. There is practically no change in $^{S}K_m$ for S-2238 over the salt concentration range explored, regardless of the particular salt used (see Figure 3). On the other hand, a small but significant change in $^{S}k_{cat}$ is observed that is also dependent on salt conditions (see Figure 4). The maximum value of $^{S}k_{cat}$ at a given value of $a_{\pm}$ is obtained with NaCl, and no change is observed upon substitution of the anion. A significant (50%) decrease in $^{S}k_{cat}$ is observed in the presence of KCl, and the same effect is quantitatively obtained upon substitution of the anion. These results too are consistent with the predominance of specific ionic interactions. The absence of salt effects on $^{S}K_m$ may not seem to support this conclusion. However, it should be pointed out that significant and specific salt effects on $^{S}K_m$ for S-2238 are seen at the same pH, but at 25 °C (Di Cera et al., 1991). The temperature dependence

Table II: Best-Fit Values of $^{S}K_m$, $^{S}k_{cat}$ and $^{F}K_m$ As Obtained from Global Analysis of Competition Experiments under Conditions of 1 nM Human α-Thrombin, 50 mM Tris, and 0.1% PEG 8000, pH 7.5 at 37 °C, in the Presence of Different Salts As Indicated[a]

[NaCl] (M)	$^{S}K_m$ (μM)	$^{S}k_{cat}$ (s^{-1})	$^{F}K_m$ (μM)	$[F_0]$ (μM)	σ (s^{-1})
0.050	10.3 ± 0.4	130.8 ± 1.5	5.5 ± 1.0	3.8	3.1
0.062*	21.9 ± 0.6	203.3 ± 1.8	5.8 ± 0.6	3.9	3.0
0.075	9.8 ± 0.3	124.1 ± 1.0	6.9 ± 0.9	4.4	2.6
0.087*	21.1 ● 0.5	201.5 ± 1.5	7.6 ± 0.8	3.6	2.8
0.100	10.7 ± 0.4	157.1 ± 1.8	8.3 ± 1.0	4.0	2.6
0.125*	20.1 ± 0.4	204.7 ± 1.3	9.4 ± 0.5	5.9	2.1
0.150	9.0 ± 0.3	172.9 ± 1.5	12.4 ± 1.6	6.0	3.0
0.175*	19.8 ± 0.4	217.2 ± 1.2	12.6 ± 0.8	9.5	2.4
0.200*	20.5 ± 0.4	204.2 ± 1.1	14.6 ± 1.0	6.8	1.9
0.250	7.5 ± 0.1	150.4 ± 0.6	13.3 ± 1.1	5.7	1.6
0.300*	20.0 ± 0.5	239.7 ± 1.8	16.6 ± 1.4	9.8	3.1
0.350	6.5 ± 0.3	183.3 ± 1.9	18.7 ± 4.4	7.2	5.1
0.400*	17.1 ± 0.3	220.1 ± 1.4	20.5 ± 2.0	7.2	2.3
0.500	8.1 ± 0.3	164.0 ± 1.3	29.2 ± 6.3	7.8	3.3
[NaBr] (M)	$^{S}K_m$ (μM)	$^{S}k_{cat}$ (s^{-1})	$^{F}K_m$ (μM)	$[F_0]$ (μM)	σ (s^{-1})
0.050	10.6 ± 0.3	141.0 ± 1.2	8.4 ± 1.5	4.7	2.5
0.075	10.9 ± 0.3	149.6 ± 1.1	10.9 ± 1.5	5.5	2.5
0.100	11.4 ± 0.3	168.6 ± 1.3	14.1 ± 1.8	6.3	2.5
0.150	8.9 ± 0.2	169.2 ± 1.2	19.7 ± 3.5	6.5	2.9
0.200	7.8 ± 0.2	170.7 ± 1.0	24.7 ± 3.6	8.2	2.6
0.300	8.7 ± 0.2	171.0 ± 1.0	34.7 ± 5.7	8.4	2.4
0.400	8.9 ± 0.3	169.1 ± 1.2	43.5 ± 10.5	9.8	3.2
[KCl] (M)	$^{S}K_m$ (μM)	$^{S}k_{cat}$ (s^{-1})	$^{F}K_m$ (μM)	$[F_0]$ (μM)	σ (s^{-1})
0.050	10.4 ± 0.4	91.6 ± 0.9	10.7 ± 1.9	7.2	1.7
0.075	10.4 ± 0.2	96.1 ± 0.6	16.4 ± 2.0	5.9	1.3
0.100	10.8 ± 0.3	108.7 ± 0.7	20.1 ± 2.5	7.0	1.5
0.150	10.1 ± 0.2	117.0 ± 0.6	20.7 ± 2.1	7.6	1.4
0.200	9.8 ± 0.2	120.2 ± 0.6	25.3 ± 2.5	9.3	1.4
0.300	8.2 ± 0.2	122.1 ± 0.7	30.0 ± 4.8	8.4	1.8
0.400	8.7 ± 0.3	136.0 ● 1.3	40.5 ± 12.2	9.5	3.4
[KBr] (M)	$^{S}K_m$ (μM)	$^{S}k_{cat}$ (s^{-1})	$^{F}K_m$ (μM)	$[F_0]$ (μM)	σ (s^{-1})
0.050	11.2 ± 0.3	93.0 ± 0.6	12.7 ± 1.6	5.0	1.3
0.075	10.5 ± 0.2	96.3 ± 0.5	17.2 ± 1.9	6.2	1.2
0.100	10.3 ± 0.2	101.4 ± 0.5	19.3 ± 1.9	8.1	1.2
0.175	10.1 ± 0.2	115.2 ± 0.6	23.7 ± 2.5	8.4	1.3
0.250	9.2 ± 0.3	127.0 ± 1.1	28.7 ± 6.3	7.4	2.5
0.350	10.1 ± 0.2	125.7 ± 0.6	38.3 ± 3.7	13.3	1.4
0.400	10.7 ± 0.3	130.8 ± 0.9	42.1 ± 10.0	7.9	2.1

[a] Errors were computed by *F*-testing at the cutoff of one standard deviation (68%). σ is the standard error of the fit. The maximum concentration of fibrinogen used is given as $[F_0]$. The synthetic substrate S-2238 was used in all experiments, except those indicated by an asterisk, where Chromozym-TH was used.

of salt effects is again a clear demonstration of the specific nature of ionic interactions that modulate thrombin activity.

A thorough examination of the validity and robustness of the experimental strategy based on competition experiments has been carried out by means of Monte Carlo simulations. The Monte Carlo has been designed to specifically address two basic aspects of the measurements reported in this study: first, whether it would be possible to resolve $^{F}K_m$ from measurements taken over a fibrinogen concentration range that does not bridge the $^{F}K_m$ value; second, whether the results of our analyses are consistent with the predictions of a simulation study where "experimental error" is truly random and no systematic error is present. Interest in the first point arises from the fact that fibrinogen has a narrow solubility range (Doolittle, 1973, 1984). Interest in the second point is due to the fact that velocity measurements of synthetic substrate hydrolysis may be affected by systematic errors, in view of the presence of scattering arising from fibrin polymerization. The

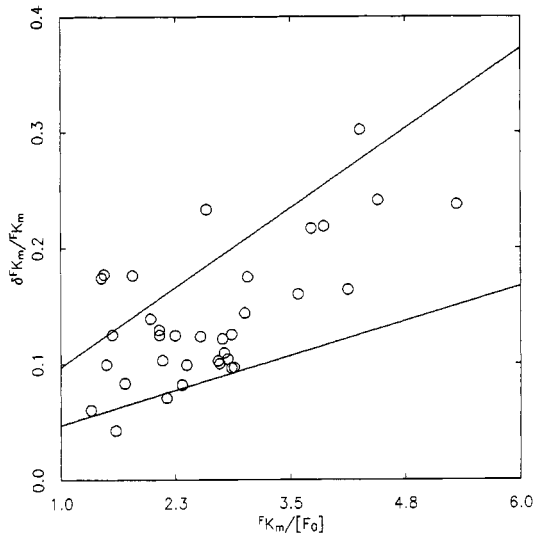

FIGURE 5: Comparison of the predictions of the Monte Carlo simulation discussed in the text with actual experimental results. The two straight lines interpolate the results of the Monte Carlo simulations with 1% (bottom line) and 2% (top line) error. Errors were simulated according to eq 4 in the text and represent the ratio between ζ and $^S k_{cat}$. For any given error, the values of $\delta^F K_m/^F K_m$ were computed from the ratio of the standard deviation and the mean of the distribution of 10 000 determinations for each of 20 different values of maximum fibrinogen concentration, $[F_0]$. The Monte Carlo simulations define a range to predict the relative error on $^F K_m$ once the ratio $^F K_m/[F_0]$ is known, given an experimental error in the range 1–2%. Actual experimental results are depicted by circles. Each point was computed from the results listed in Table II and represents the relative error on $^F K_m$, given as the ratio between the error and best-fit value of this parameter, as a function of the ratio $^F K_m/[F_0]$. The ratio $\sigma/^S k_{cat}$ (see Table II) gives the experimental error of the actual experimental measurements, which is within the 1–2% range for almost all (30 out of 35) determinations.

Monte Carlo simulation was designed and carried out along lines described in detail elsewhere (Di Cera, 1992). Velocity measurements of synthetic substrate hydrolysis were simulated according to the equation:

$$v = e_T \frac{^S k_{cat}[S]}{^S K_m\{1 + [F]/^F K_m\} + [S]} + \epsilon \qquad (4)$$

Here ϵ is a pseudorandom error with zero mean and a standard deviation equal to ζ, given by $\epsilon = \zeta\sqrt{-2 \ln (RND_1)} \cos (2\pi RND_2)$ (Box & Muller, 1958), where RND_1 and RND_2 are two random numbers in the range 0–1. Values of e_T = 1 nM, $^S k_{cat}$ = 150.4 s^{-1}, $^S K_m$ = 7.5 μM, and $^F K_m$ = 13.3 μM were used in all simulations. These values correspond to the best-fit values determined experimentally under conditions of 0.25 M NaCl (see Tables I and II). Velocity measurements were simulated according to eq 4 in the form taken experimentally, i.e., in a 7 × 8 matrix using seven different substrate concentrations (scaled by a factor of 2) and eight different fibrinogen concentrations (scaled by a factor of 1.5), one of which was equal to zero. All data points were analyzed together according to eq 3. Twenty different values of maximum fibrinogen concentration were used, in the range $^F K_m/6 - {}^F K_m$, as well as 2 different values of experimental error, ζ, corresponding to 1% and 2% of the simulated $^S k_{cat}$ value. For each 1 of the 40 combinations of maximum fibrinogen concentration and experimental error, 10 000 sets of 56 data points were generated and analyzed according to eq 3, and the resulting best-fit estimates of $^S k_{cat}$, $^S K_m$, and $^F K_m$ were collected for statistical evaluation to compute the mean and standard deviation associated with each parameter. The difference between the mean values obtained from the Monte Carlo and the simulated ones gives the bias for each parameter and was found to be less than 1% in all cases. The results of the Monte Carlo can be used to predict the dependence of the percent error of $^F K_m$, obtained as the ratio between the standard deviation and the mean of the distribution of parameter values, on the ratio $^F K_m/[F_0]$, where $[F_0]$ is the maximum fibrinogen concentration. Analysis of the results of the Monte Carlo yields the two straight lines shown in Figure 5, corresponding to 1% (lower curve) and 2% (upper curve) experimental error. Circles in Figure 5 depict the results of all experimental measurements reported in this study. The striking agreement between actual experimental measurements and the predictions of the Monte Carlo simulation demonstrates that the strategy of collecting data in a 7 × 8 matrix of substrate and fibrinogen concentrations is very reliable and robust when the experimental error is in the 1–2% range, as typically found in our measurements (see Table II). It also shows that no significant systematic error arises in our measurements from complicating effects due to scattering, since a perfect agreement is found between actual data and simulated measurements without any systematic trend.

Table III: Best-Fit Values of t_∞ and $\alpha^F K_m/^F k_{cat}$ (See eq 5 in the Text) As Obtained from Analysis of the Clotting Time as a Function of Thrombin Concentration (See Also Figure 6)[a]

salt	t_∞ (s)	$\alpha^F K_m/^F k_{cat}$ (nM s^{-1})	σ (s)	ρ	ρ'
NaCl	2.0 ± 1.2	242.2 ± 7.8	3.6	1.0 ± 0.0	1.0 ± 0.0
NaBr	7.6 ± 2.5	400.6 ± 8.7	4.0	1.7 ± 0.3	1.7 ± 0.7
KCl	0.1 ± 1.5	725.7 ± 15.8	6.0	3.0 ± 0.4	2.4 ± 0.9
KBr	2.6 ± 1.8	1359.3 ± 21.1	3.4	5.6 ± 1.0	2.3 ± 0.8

[a] Under experimental conditions of 0.25 μM fibrinogen, 50 mM Tris, and 0.1% PEG 8000, pH 7.5 at 37 °C, in the presence of 0.1 M salt concentration as indicated. σ is the standard eror of the fit. ρ is the ratio between the values of $\alpha^F K_m/^F k_{cat}$ for a given salt relative to NaCl. ρ' is the ratio between the values of $^F K_m$ for a given salt relative to NaCl (see Table II).

Further support to the results obtained from competition experiments comes from the analysis of the effect of different salts on the clotting curve. We have recently shown that quantitative information can be obtained on the enzymatic steps triggering clot formation from a phenomenological analysis of the clotting curve (De Cristofaro & Di Cera, 1991). In particular, we have pointed out that the clotting time, t_c, is directly proportional to the ratio K_m/V_{max} for fibrinogen when the clotting curve is measured in the presence of fibrinogen concentrations small compared to $^F K_m$. Under these conditions, t_c can be written as

$$t_c = t_\infty + \alpha(^F K_m/^F k_{cat}) e_T^{-1} \qquad (5)$$

where t_∞ is the asymptotic clotting time at infinite thrombin concentration, $^F k_{cat}$ is the value of k_{cat} for fibrinogen, and α is a constant. A plot of t_c versus the inverse thrombin concentration is expected to be linear. The results obtained in the presence of the four different salts used in the competition experiments are shown in Figure 5 and confirm this expectation. Again, a drastic difference is seen with different salts, most notably in the slope of the curves. The best-fit values of the parameters involved in eq 5 are given in Table III. The slope of each curve in Figure 6 gives the thrombin concentration for which $t_c - t_\infty$ = 1 s. This quantity changes by a factor of 5.6 when NaCl is replaced by KBr, and by a factor of 3.0 when NaCl is replaced by KCl. With the exception of KBr, these changes are practically identical to those observed in the case of $^F K_m$ from the competition experiments, as demonstrated by the similarity of ρ and ρ' values listed in Table III. This suggest that the parameter α in eq 5, which is related

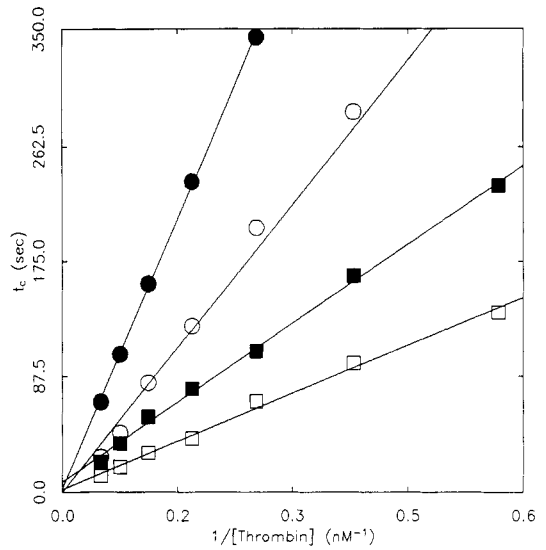

FIGURE 6: Values of the clotting time, t_c, as a function of the inverse thrombin concentration obtained in the presence of 0.1 M (□) NaCl, (■) NaBr, (○) KCl, or (●) KBr. Experimental conditions are 0.25 μM human fibrinogen, 50 mM Tris, and 0.1% PEG 8000, pH 7.5 and 37 °C. Straight lines were drawn according to eq 5 in the text using the best-fit parameter values listed in Table III.

to the fraction of fibrinogen converted to fibrin at the clotting time (De Cristofaro & Di Cera, 1991), as well as $^{F}k_{cat}$ may change very little with different salts. However, the alternative possibility that these two parameters may change in an opposite fashion with different salts is equally likely. The most important aspect of the data shown in Figure 6 is that the drastic changes observed with different salts occur without any change in the ionic strength of the medium, and this points out that specific ion effects play a major role in the modulation of thrombin–fibrinogen interaction in vivo. Of particular importance is the observation that the clotting time is minimal in the presence of the physiological salt NaCl and increases significantly when Na^+ is replaced by K^+, even in the presence of the physiological anion Cl^-. The relative levels of all these ions in the blood may therefore be critical for the control of thrombin–fibrinogen interaction leading to clot formation.

Discussion

Outstanding treatments of the basic thermodynamic principles involved in ion effects (Lewis & Randall, 1961; Tanford, 1962; Manning, 1969; Record et al., 1978) have long pointed out that a meaningful characterization of ion effects on macromolecular interactions can only be accomplished by experimental studies conducted with different salts. The strategy developed in this study is perfectly consistent with these theoretical considerations. The competition experiments of substrate hydrolysis in the presence of fibrinogen reported in this study have revealed some quantitative aspects of thrombin–fibrinogen interaction under conditions that are relevant to the situation in vivo. Three parameters have been resolved with good accuracy from global analysis of experimental data obtained over a range of substrate and fibrinogen concentrations. Two parameters, $^{S}K_m$ and $^{S}k_{cat}$, quantify thrombin amidase activity toward the synthetic substrate, while the third parameter, $^{F}K_m$, represents the Michaelis–Menten constant for fibrinogen. It is of interest to compare the values of $^{F}K_m$ obtained in this study with those reflecting the release of fibrinopeptide A, as obtained by HPLC under similar solution conditions. Overwhelming experimental evidence obtained with human or bovine thrombin and fibrinogen shows that the release of fibrinopeptide A precedes that of fibrinopeptide B (Higgins et al., 1983; Hofsteenge et al., 1986, 1988; Mihaly, 1988b; Schmitz et al., 1991). Also, the increase in turbidity in the clotting assay observed up to the clotting time occurs well before any appreciable release of fibrinopeptide B can be detected (Mihaly, 1988a). In view of these findings, it is not surprising that the value of $^{F}K_m = 9.4 \pm 0.5$ μM, obtained in this study in the presence of 0.125 M NaCl, compares very well with the values of K_m for the release of fibrinopeptide A as determined by HPLC under similar solution conditions. These values range from 6.9 to 11.4 μM (Higgins et al., 1983; Hofsteenge et al., 1986, 1988; Schmitz et al., 1991), with an average value of 9.2 ± 2.0 μM. Unlike HPLC assays, the competition experiments described in this study can only provide estimates of $^{F}K_m$, but not $^{F}k_{cat}$. The method based on competition experiments is however much simpler than the HPLC assays and provides estimates of $^{F}K_m$ that are more accurate. It provides an effective strategy to explore the properties of thrombin–fibrinogen interaction under a wide variety of solution conditions, which is a necessary condition to assess the thermodynamic driving forces responsible for this physiologically important reaction in a quantitative way. Also, since $^{F}K_m$ is related to the fibrinogen dissociation constant, unlike $^{F}k_{cat}$ that only reflects acylation (see eq 2), measurements of $^{F}K_m$ are highly desirable and absolutely critical to assess the thermodynamic components underlying thrombin–fibrinogen interaction.

A fundamental aspect of thrombin amidase activity should be brought out in this connection. In the hydrolysis of amide substrates by serine proteases, acylation is rate-limiting (Fersht, 1985). This has been verified experimentally for thrombin interaction with the synthetic substrate S-2238 over a wide range of solution conditions (Di Cera et al., 1991) and fully justifies our analysis of competition experiments in terms of the kinetic eq 2. We have also shown that $^{S}K_m$ for S-2238 corresponds to the substrate dissociation constant (Di Cera et al., 1991). Once the specific nature of ion effects has been established by comparative studies conducted in the presence of different salts, the dependence of the logarithm of the substrate dissociation constant, or its equivalent quantity $^{S}K_m$, with respect to the logarithm of the mean ion activity $a_\pm$ can be given a direct thermodynamic interpretation. In this case, the slope $\Delta\nu = -\mathrm{d} \ln {}^{S}K_m / \mathrm{d} \ln a_\pm$ equals the net number of cations and anions exchanged upon substrate binding to the enzyme (Record et al., 1978; Lohman, 1985). Ions are uptaken or released upon substrate binding depending on whether $\Delta\nu$ is positive or negative. The results reported in this study show that the total number of ions exchanged upon substrate binding to the enzyme is practically zero under experimental conditions of physiological interest. The effects seen on $^{F}K_m$ are, however, quite different. Since fibrinogen is an amide substrate for thrombin, acylation is expected to be rate-limiting, as in the case of synthetic substrates (see eq 2). However, this fact per se does not guarantee that $^{F}K_m$ equals the dissociation constant for fibrinogen, as in the case of the synthetic substrate S-2238. More information needs to be collected from studies conducted at different pHs and temperatures (Di Cera et al., 1991) in order to assess whether the Michaelis–Menten constant $^{F}K_m$ directly reflects the equilibrium dissociation constant of fibrinogen. In the absence of such information, we can only speculate on the possible thermodynamic significance of the data reported in this study and summarized in Figure 3. If $^{F}K_m$ corresponds to the fibrinogen dissociation constant, then the results reported in this study show that ions are released upon fibrinogen binding to thrombin to a different extent, which depends on the particular salt present in solution.

The maximum linkage is observed with NaBr, followed by NaCl, KCl, and KBr in order. Up to 0.90 ion can be released upon fibrinogen binding to thrombin. These ions can be released from the enzyme and/or from fibrinogen upon thrombin–fibrinogen interaction. Interestingly, it is clear from the data shown in Figure 3 that significant interactions must exist between cation and anion binding sites, regardless of their location. This is because the differential effect of anions is cation-dependent and vice versa, while in the absence of interactions the difference between NaCl and NaBr would be the same as that between KCl and KBr. The existence of interactions between cation and anion binding sites may suggest, to a first approximation, that these sites are structurally close together. A simple picture can be envisaged as follows. One can assume that fibrinogen binding to thrombin requires the formation of salt bridges that involve positively charged residues in the FRS and negatively charged residues in the fibrinogen domain that interacts with the FRS. The positive charges in the FRS may provide a natural binding domain for small anions, and, conversely, small cations can preferentially interact with the domain of fibrinogen complementary to the FRS. Different ions may bind with different affinities. In this picture, both anions and cations must be released to expose the charged groups responsible for thrombin–fibrinogen interaction. The extent of release depends on the binding affinity and gives rise to the dependence of $^{F}K_{m}$ observed experimentally. Also, the release of anions/cations from one side would favor the release of cations/anions from the other side by simple electrostatic repulsion. This picture would provide a simple explanation for the results shown in Figure 3, although alternative interpretations cannot be ruled out at this stage. If $^{F}K_{m}$ is not equal to the fibrinogen dissociation constant, then the interpretation of the data reported in Figure 3 in terms of linkage effects is more difficult. If fibrinogen is a sticky substrate for thrombin, i.e., if the acylation rate $^{F}k_{2}$ is faster than or comparable to the dissociation rate $^{F}k_{-1}$, then $^{F}K_{m}$ equals the dissociation constant, $^{F}K_{d}$, times a correcting factor equal to $1 + {}^{F}k_{2}/{}^{F}k_{-1}$. In this case, $^{F}K_{m}$ provides only an upper limit to the true dissociation constant. The derivative $d \ln {}^{F}K_{m}/d \ln a_{\pm}$ also reflects the effect of salts on the individual kinetic rates $^{F}k_{2}$ and $^{F}k_{-1}$, and hence the simple molecular interpretation of the facts provided above may be valid only under further simplifications.

No matter which interpretation we choose for $^{F}K_{m}$, the most important implication drawn from the results of this study is that specific ion effects modulate thrombin–fibrinogen interaction under experimental conditions of physiological interest. Small ions can therefore be considered as allosteric effectors of thrombin function in vivo. This result, along with previous findings on the extreme sensitivity of thrombin amidase and esterase activity to salt conditions (Roberts et al., 1969; Workman & Lundblad, 1978; Orthner & Kosow, 1980; Landis et al., 1981; Di Cera et al., 1991), clearly demonstrates that specific ion binding effects are major driving forces for thrombin–fibrinogen interaction. These thermodynamic components should be given much consideration in any future analysis of the mechanism of action of synthetic inhibitory peptides, as well as natural competitive inhibitors such as hirudin, that bridge-bind to the FRS and the catalytic pocket like fibrinogen. A thorough experimental investigation of the effect of these inhibitors according to the strategy described in this study is necessary in order to characterize those aspects of the linkage between ion release and macromolecular binding to the FRS that are common to different molecules and those that are peculiar of fibrinogen.

ACKNOWLEDGMENTS

We are grateful to Dr. John Fenton, II, for kindly providing human thrombin.

Registry No. S-2238, 62354-65-8; Na, 7440-23-5; K, 7440-09-7; Br, 24959-67-9; Cl, 16887-00-6; α-thrombin, 9002-04-4; Chromozym-TH, 86890-95-1.

REFERENCES

Bode, W., Baumann, U., Huber, R., Stone, S. R., & Hofsteenge, J. (1989) *EMBO J. 8*, 3467–3476.

Box, G. E. P., & Muller, M. E. (1958) *Ann. Math. Stat. 29*, 610–615.

Braun, P. J., Hofsteenge, J., Chang, J.-Y., & Stone, S. R. (1988) *Thromb. Res. 50*, 273–283.

Chase, T., & Shaw, E. (1967) *Biochem. Biophys. Res. Commun. 29*, 508–514.

Church, F. C., Pratt, C. W., Noyes, C. M., Kalayanamit, T., Sherrill, G. B., Tobin, R. B., & Meade, J. B. (1989) *J. Biol. Chem. 264*, 18419–18425.

De Cristofaro, R., & Di Cera, E. (1991) *J. Protein Chem. 10*, 455–468.

Deutsch, D. G., & Mertz, E. T. (1970) *Science 170*, 1095–1096.

Di Cera, E. (1992) *Methods Enzymol. 210*, 68–87.

Di Cera, E., Andreasi Bassi, F., & Arcovito, G. (1989) *Biophys. Chem. 34*, 29–48.

Di Cera, E., De Cristofaro, R., Albright, D. J., & Fenton, J. W., II (1991) *Biochemistry 30*, 7913–7924.

Dietler, G., Kanzig, W., Haberli, A., & Straub, P. W. (1986) *Biopolymers 25*, 905–929.

Di Maio, J., Gibbs, B., Munn, D., Lefebvre, J., Ni, F., & Konishi, Y. (1990) *J. Biol. Chem. 265*, 21698–21703.

Doolittle, R. F. (1973) *Adv. Protein Chem. 27*, 1–109.

Doolittle, R. F. (1984) *Annu. Rev. Biochem. 53*, 195–236.

Engvall, E., Ruoslahti, E., & Miller, E. J. (1978) *J. Exp. Med. 147*, 1584–1595.

Fenton, J. W., II, Fasco, M. J., Stackrow, A. B., Aronson, D. L., Young, A. M., & Finlayson, J. S. (1977) *J. Biol. Chem. 252*, 3587–3598.

Fersht, A. R. (1985) in *Enzyme Structure and Mechanism*, Freeman, New York.

Griffith, M. J. (1979) *J. Biol. Chem. 254*, 3401–3406.

Hantgan, R. R., & Hermans, J. (1979) *J. Biol. Chem. 254*, 11272–11281.

Higgins, D. L., Lewis, S. D., & Shafer, J. A. (1983) *J. Biol. Chem. 258*, 9276–9282.

Hofsteenge, J., Taguchi, H., & Stone, S. R. (1986) *Biochem. J. 237*, 243–251.

Hofsteenge, J., Braun, P. J., & Stone, S. R. (1988) *Biochemistry 27*, 2144–2151.

Laki, K., & Gladner, J. A. (1964) *Physiol. Rev. 44*, 127–160.

Landis, B. H., Koehler, K. A., & Fenton, J. W., II (1981) *J. Biol. Chem. 256*, 4604–4610.

Lewis, G. N., & Randall, M. (1961) in *Thermodynamics*, McGraw-Hill, New York.

Lohman, T. M. (1985) *CRC Crit. Rev. Biochem. 19*, 191–245.

Lord, S. T., Byrd, P. A., Hede, K. L., Wei, C., & Colby, T. J. (1990) *J. Biol. Chem. 265*, 838–843.

Lundlbad, R. L., Nesheim, M. E., Straight, D. L., Sailor, S., Bowie, J., Jenzano, J. W., Roberts, J. D., & Mann, K. G. (1984) *J. Biol. Chem. 259*, 6991–6995.

Manning, G. S. (1969) *J. Chem. Phys. 51*, 924–933.

Maraganore, J. M., Bourdon, P., Jablonski, J., Ramachandran, K. L., & Fenton, J. W., II (1990) *Biochemistry 29*, 7095–7101.

Martinelli, R. A., & Scheraga, H. A. (1980) *Biochemistry 19*, 2343-2350.
Mihaly, E. (1968) *Biochemistry 7*, 208-223.
Mihaly, E. (1988a) *Biochemistry 27*, 967-976.
Mihaly, E. (1988b) *Biochemistry 27*, 976-982.
Orthner, C. L., & Kosow, D. P. (1980) *Arch. Biochem. Biophys. 202*, 63-75.
Record, M. T., Anderson, C. F., & Lohman, T. M. (1978) *Q. Rev. Biophys. 11*, 103-178.
Roberts, P. S., Burkat, R. K., & Braxton, W. E. (1969) *Thromb. Diath. Haemorrh. 21*, 105-112.
Rubinow, S. I., & Lebowitz, J. L. (1970) *J. Am. Chem. Soc. 92*, 3888-3893.
Rydel, T. J., Ravichandran, K. G., Tulinsky, A., Bode, W., Huber, R., Roitsch, C., & Fenton, J. W., II (1990) *Science 249*, 277-280.
Scheraga, H. A., & Laskowski, M. (1957) *Adv. Protein Chem. 12*, 1-131.
Schmitz, T., Rothe, M., & Dodt, J. (1991) *Eur. J. Biochem. 195*, 251-256.
Segel, L. A. (1988) *Bull. Math. Biol. 50*, 579-593.
Stone, S. R., & Hofsteenge, J. (1986) *Biochemistry 25*, 4622-4628.
Sturtevant, J. M., Laskowski, M., Donnelly, T. H., & Scheraga, H. A. (1955) *J. Am. Chem. Soc. 77*, 6168-6172.
Tanford, C. (1962) *Adv. Protein Chem. 17*, 69-165.
Workman, E. F., & Lundblad, R. (1978) *Arch. Biochem. Biophys. 185*, 544-548.

Thrombospondin Is a Slow Tight-Binding Inhibitor of Plasmin†

Philip J. Hogg,*,‡ Johan Stenflo, and Deane F. Mosher§
Department of Clinical Chemistry, University of Lund, Malmö General Hospital, S-21401 Malmö, Sweden
Received June 21, 1991; Revised Manuscript Received September 24, 1991

ABSTRACT: Thrombospondin is a multifunctional glycoprotein of platelet α-granules and a variety of growing cells. We demonstrate that thrombospondin is a slow tight-binding inhibitor of plasmin as determined by loss of amidolytic activity, loss of ability to cleave fibrinogen, and decreased lysis zones in fibrin plate assays. Stoichiometric titrations indicate that approximately 1 mol of plasmin interacts with 1 mol of thrombospondin, an unexpected result considering the trimeric nature of thrombospondin. Plasmin in a complex with streptokinase or bound to ε-aminocaproic acid is protected from inhibition by thrombospondin, thereby implicating the lysine-binding kringle domains of plasmin in the inhibition process. Thrombospondin also inhibits urokinase plasminogen activator, but more slowly than plasmin, stimulates the amidolytic activity of tissue plasminogen activator, and has no effect on the amidolytic activity of α-thrombin or factor Xa. These results, therefore, identify thrombospondin as a new type of serine proteinase inhibitor and potentially important regulator of fibrinolysis.

Thrombospondin (TSP),[1] a 450 000-dalton trimer of 150 000-dalton disulfide-bonded subunits, is a major constituent of platelet α-granules and is released upon platelet activation (Frazier, 1987). TSP is also a product of normal and transformed cells in culture, including endothelial cells (Mosher et al., 1982), smooth muscle cells (Raugi et al., 1982), fibroblasts (Jaffe et al., 1983), monocytes (Jaffe et al., 1985), and glial cells (Asch et al., 1986), and a constituent of their extracellular matrix (Jaffe et al., 1983). Embryonic tissues immunostain intensely for TSP (O'Shea & Dixit, 1988). In addition, atherosclerotic lesions exhibit marked immunostaining for TSP (Wight et al., 1985). Among known functions of TSP are binding specific to Ca^{2+} (Lawler & Simons, 1983), heparin (Dixit et al., 1984), collagen (Galvin et al., 1987), fibronectin (Lahav et al., 1984), fibrinogen (Leung & Nachman, 1982), fibrin (Bale et al., 1985), laminin (Lawler et al., 1986), plasminogen (Silverstein et al., 1984), and urokinase plasminogen activator (u-PA) (Harpel et al., 1990). Thus, TSP has the potential to play a role in tissue remodeling, development, and hemostasis.

Materials and Methods

Chemicals. H-D-Val-Leu-Lys-*p*-nitroanilide (S2251) and H-D-Ile-Pro-Arg-*p*-nitroanilide (S2288) were purchased from Kabi, Mölndal, Sweden, and *p*-nitrophenyl p-guanidinobenzoate and ε-aminocaproic acid (ε-ACA) were from Sigma Chemical Co., St. Louis, MO.

Proteins. Plasminogen was purified from fresh frozen human plasma and separated into its two carbohydrate variants according to published procedures (Castellino & Powell, 1981). Plasminogen was activated by u-PA immobilized on Sepharose 4B as described previously (Wiman & Wallén, 1973). Ac-

† This investigation was supported by the Swedish Medical Research Council and the Albert Påhlsson's Foundation. P.J.H. was supported by a Visiting Scientist Fellowship from the Swedish Medical Research Council. D.F.M. was supported by National Institutes of Health Grant HL29586.
* To whom correspondence should be addressed.
‡ Permanent address: Department of Haematology, The Prince of Wales Hospital, Randwick, NSW 2031, Australia.
§ Permanent address: Departments of Medicine and Physiological Chemistry, University of Wisconsin, Madison, WI 53706.

[1] Abbreviations: TSP, thrombospondin; S2251, H-D-Val-Leu-Lys-*p*-nitroanilide; S2288, H-D-Ile-Pro-Arg-*p*-nitroanilide; u-PA, urokinase plasminogen activator; t-PA, tissue plasminogen activator; HEPES *N*-(2-hydroxyethyl)piperazine-*N'*-2-ethanesulfonic acid; SDS-PAGE, sodium dodecyl sulfate-polyacrylamide gel electrophoresis; HBD, amino-terminal heparin binding domain of TSP; TSP(-HBD), TSP lacking the amino-terminal HBD; ε-ACA, ε-aminocaproic acid.

0006-2960/92/0431-265$03.00/0